Identifying Long-term Mortality Improvement Rates: A LiDAR Approach

Yanxin Liu, Johnny Siu-Hang Li

The 19th International Longevity Risk and Capital Markets Solutions Conference, Amsterdam
September 2024

Outline

Background

Mortality Improvement

- Gradual reduction in death rates over time.
- Factors contributing to mortality improvement:
  - advancements in healthcare,
  - better living conditions,
  - improved public health measures,
  - advances in medical technology,
  - increased awareness of healthier lifestyles
- The pros: longer and healthier life
- The cons: strain on life annuity providers, pension and social security systems
  - Longer lifespans $\Rightarrow$ longer periods $\Rightarrow$ funding shortfalls $\Rightarrow$ cuts in benefits if not properly adjusted

Mortality Improvement Scales

Practitioners have developed mortality improvement scales to determine an allowance of future mortality improvement

- One-dimensional scales (age only):
  - North America:
    Scale AA (1994), VBT (2002), Scale BB (2012)
  - United Kingdom:
    the “80” Series (1990), the “92” Series (1999)
- Two-dimensional scales (both age and year):
  - North America:
    CPM-B (2014), MP-2014 to MP-2021.
  - United Kingdom:
    the “phototype model” (2009), the CMI model (2009 to 2023)

General Principles of 2D Scales

- A three component approach
- A **short-term** scale for the near future:
  - Generally high short-term rates to reflect the rapid mortality improvement in recent decades
- A **long-term** scale for the distant future:
  - (Very) low long-term rates on grounds that rapid mortality improvement will not last forever
- A **mid-term** scale for the transitional phase:
  - An interpolation between long- and short-term rates

MP-2021 (SOA)

- Developed by the SOA's Retirement Plans Experience Committee (RPEC) for a broad range of retirement programs in the US.
- First released in 2014 and updated annually until 2021.
- **Short-term** scale (up to 2017, a two-year step back):
  - SSA probabilities of death, smoothed with order-3 Whittaker-Henderson graduation
- **Long-term** scale (2037 and beyond):
  - flat 1.35% rate to age 62, decreasing linearly to 1.10% at age 80, further decreasing linearly to 0.40% at age 95, and then decreasing linearly to 0.00% at age 115
- **Mid-term** scale (2018-2036):
  - A "double-cubic interpolation"

MP-2021 (SOA)

- Developed by the SOA's Retirement Plans Experience Committee (RPEC) for a broad range of retirement programs in the US.
- First released in 2014 and updated annually until 2021.
- **Short-term** scale (up to 2017, a two-year step back):
  - SSA probabilities of death, smoothed with order-3 Whittaker-Henderson graduation
- **Long-term** scale (2037 and beyond):
  - flat 1.35% rate to age 62, decreasing linearly to 1.10% at age 80, further decreasing linearly to 0.40% at age 95, and then decreasing linearly to 0.00% at age 115
- **Mid-term** scale (2018-2036):
  - A "double-cubic interpolation"

Challenges

- Determined by either expert judgments or by making reference to the assumptions used in other jurisdictions.

Time Period	Age 55-64	Age 65-74	Age 75-84	Age 85-94
1940-2017	1.29%	1.19%	1.08%	0.75%
1950-2017	**1.33%**	**1.24%**	**1.09%**	**0.71%**
1960-2017	1.45%	1.36%	1.13%	0.73%
1970-2017	1.48%	1.43%	1.09%	0.53%
1980-2017	1.39%	1.52%	1.09%	0.40%
1940-1980	0.99%	0.94%	1.06%	0.87%
1950-1990	1.13%	0.99%	1.09%	0.97%
1960-2000	1.48%	1.18%	1.12%	0.94%
1970-2010	1.63%	1.38%	1.05%	0.49%

Source: Mortality Improvement Scale MP-2021.

- Changes in the time period can influence the results.

Research Objective

- To propose a new method for the identification of long-term mortality improvement rates.

A LiDAR Approach

What is LiDAR?

- LiDAR stands for Light Detection and Ranging.
- It uses light pulses to measure distance of objects.
- LiDAR is widely used in many areas such as mapping, geodesy, agriculture, autonomous vehicles, etc.

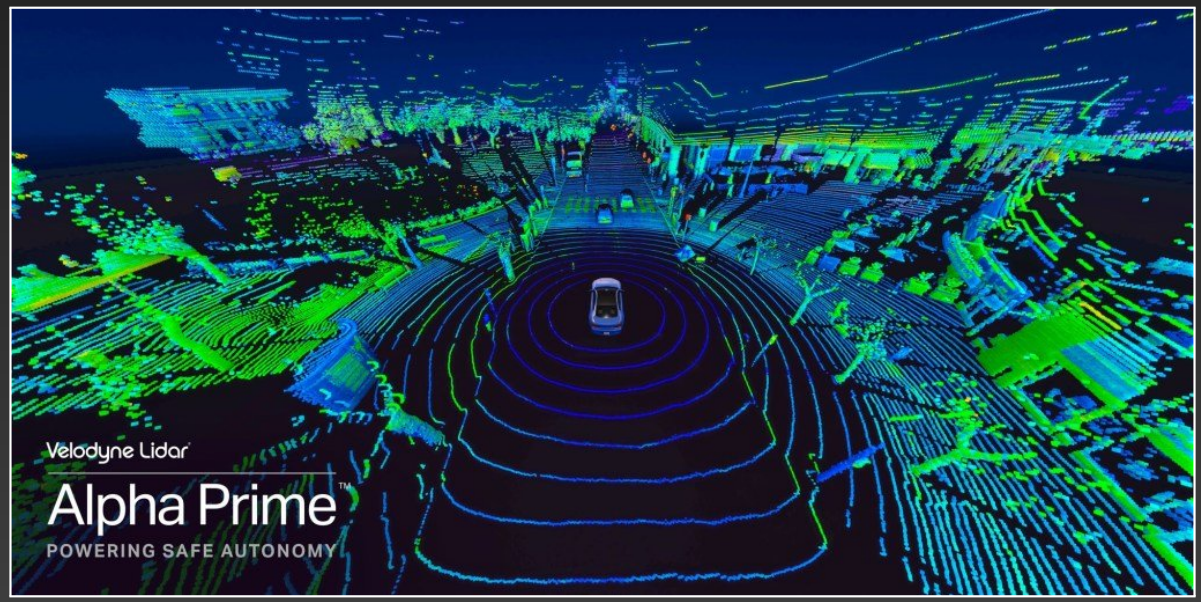

A 3D point cloud created by the Velodyne LiDAR.

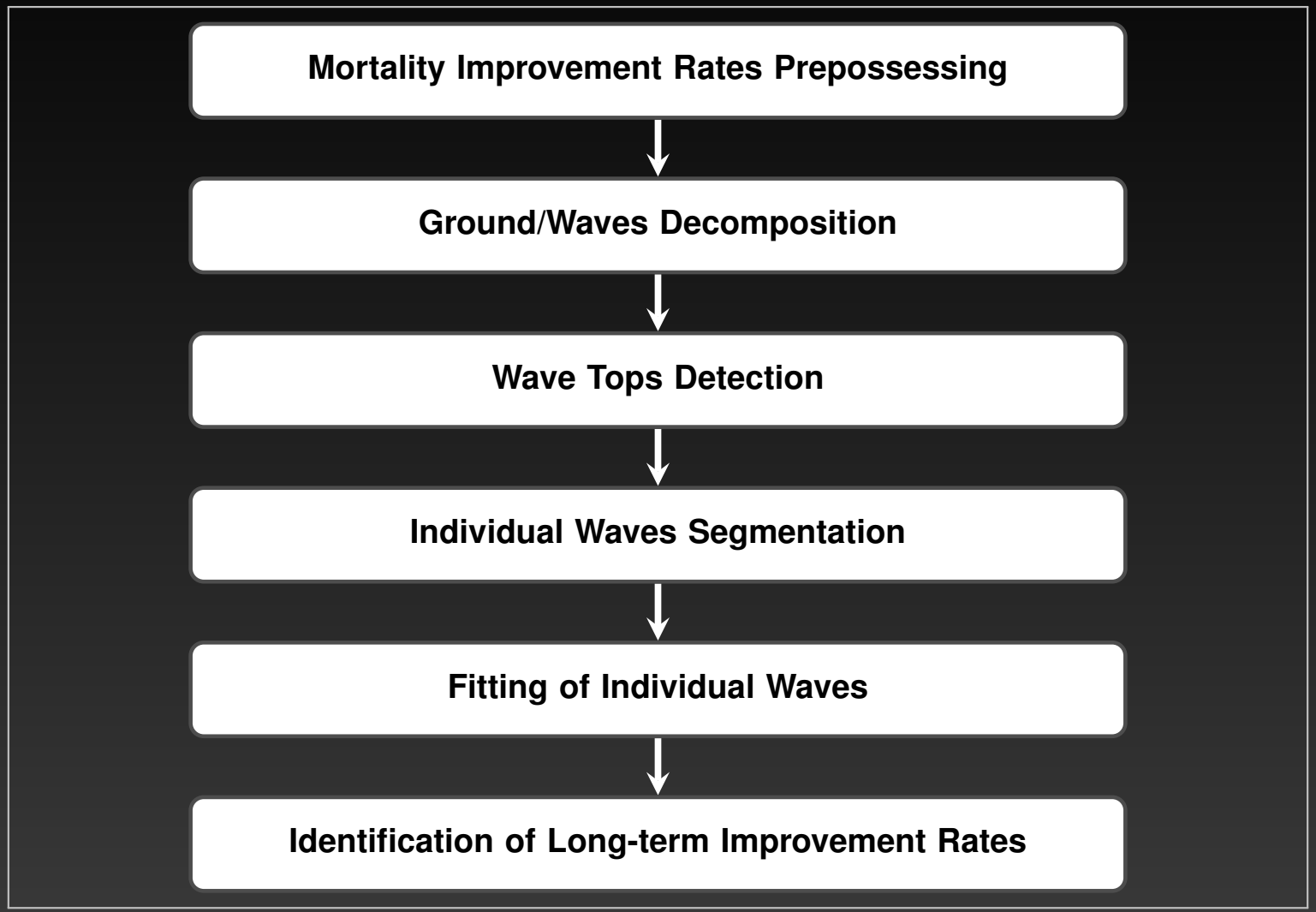

Figure: A flow diagram of the proposed LiDAR approach for the identification of long-term improvement rates.

Notations

- Let us use $D_{x,t}$ and $E_{x,t}$ to denote the death counts and exposures for age x in year t, respectively.
- The raw central death rates $m_{x,t}$ is calculated by

$$m_{x,t} = \frac{D_{x,t}}{E_{x,t}}.$$

- The (log) mortality improvement rates $Z_{x,t}$ is defined by

$$Z_{x,t} = \log\left(\frac{m_{x,t-1}}{m_{x,t}}\right) = \log(m_{x,t-1}) - \log(m_{x,t}) \qquad (1)$$

- Note: $Z_{x,t} > 0$ refers to the case that mortality improves for individuals age x from year $t-1$ to year t, while $Z_{x,t} < 0$ refers to the case of mortality deterioration.

A LiDAR Approach

Stage 1: Mortality Improvement Rates Prepossessing

Stage 1: Mortality Improvement Rates Prepossessing

- No sensible pattern is detected when considering the raw mortality improvement rates
- The prepossessing of mortality improvement rates is crucial in revealing the pattern from the raw data.
- We prepossess the data by fitting $Z_{x,t}$ to a 2-dimensional P-splines regression (Currie et al., 2004)
- We denote the resulting smoothed rates by $\tilde{Z}_{x,t}$.

Numerical Illustration

Data: U.S. males population, ages 60-89, years 1960-2019

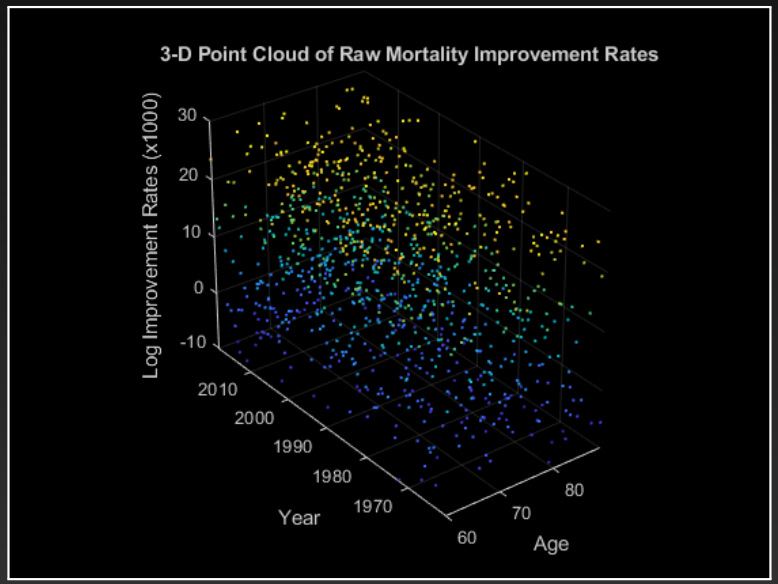

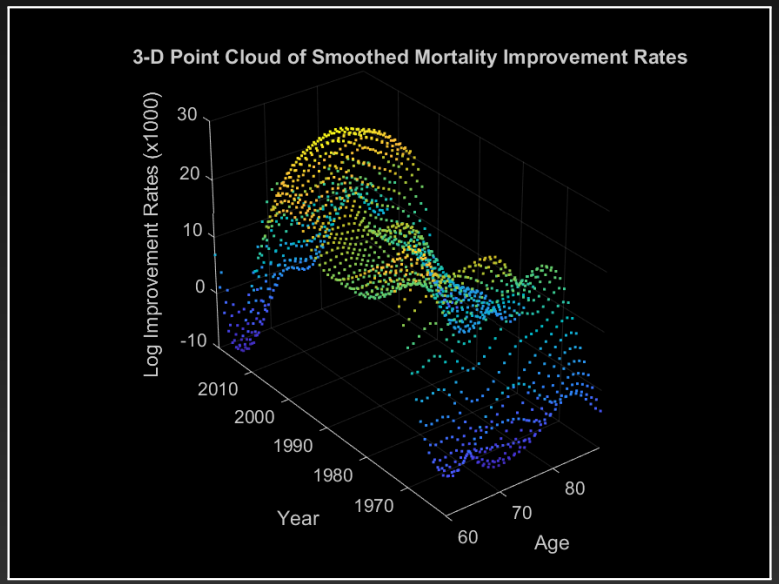

Figure: Comparison between the raw mortality improvement rates and smoothed mortality improvement rates.

Numerical Illustration

Data: U.S. males population, ages 60-89, years 1960-2019

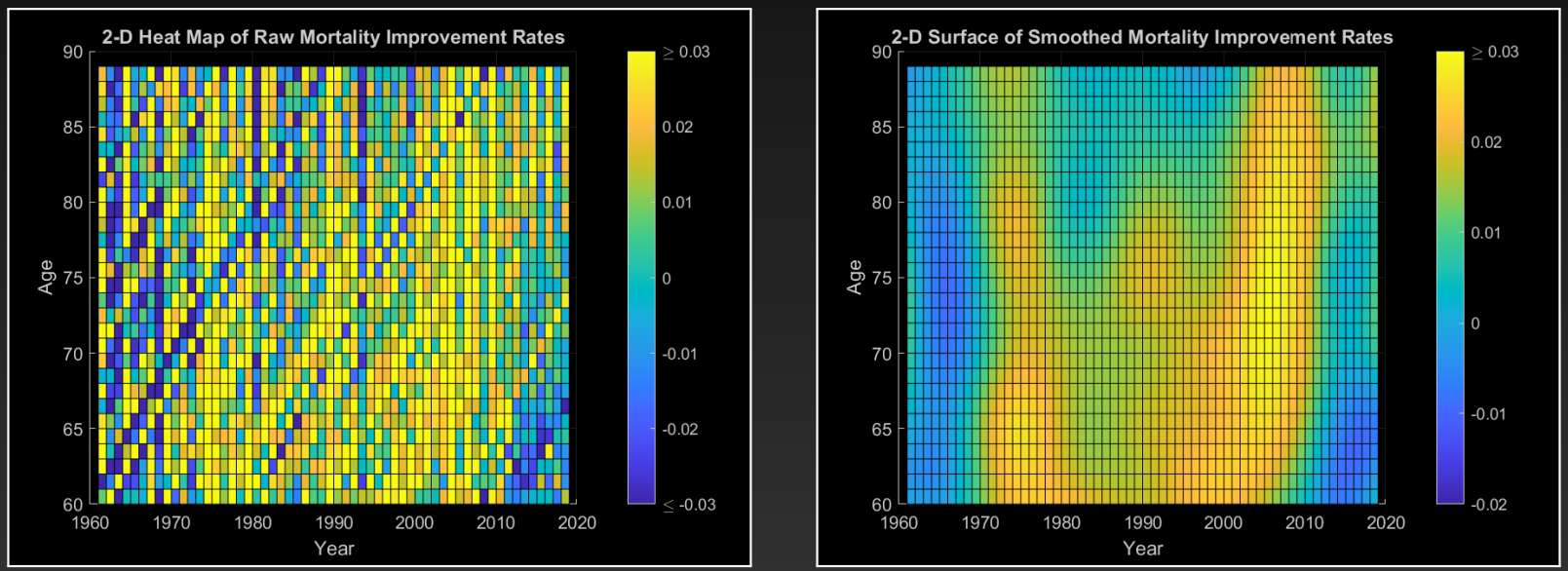

Figure: Comparison between the raw mortality improvement rates and smoothed mortality improvement rates.

A LiDAR Approach

Stage 2: Ground/Waves Decomposition

Stage 2: Ground/Waves Decomposition

- Smoothed improvement rates are decomposed into
  - ground layer: long-term background improvement
  - nonground layer: short-term improvement/deterioration
- The *simple morphological filter* (SMRF) algorithm is used.
  - Designed to address terrain classification of LiDAR data.
- Implementation of the SMRF Method (Pingel et al., 2013)
  - Progressive use of the *morphological opening* operation on the mortality improvement surface.

Morphological Opening

- *Morphological opening* operation is a technique used in image processing to remove small objects from an image while maintaining the size and shape of larger objects.
- It includes an *erosion filter*, followed by a *dilation filter*.
  - Erosion filter: pulls data points with relative high values to their local minima
  - Dilation filter: drags points with relative low values to their local maxima

Illustration of Morphological Erosion and Dilation

- The erosion of image A by the structuring element B is denoted as

$$A \ominus B$$

- The dilation of A by the structuring element B is denoted as

$$A \oplus B$$

- Illustration of *erosion* and *dilation*

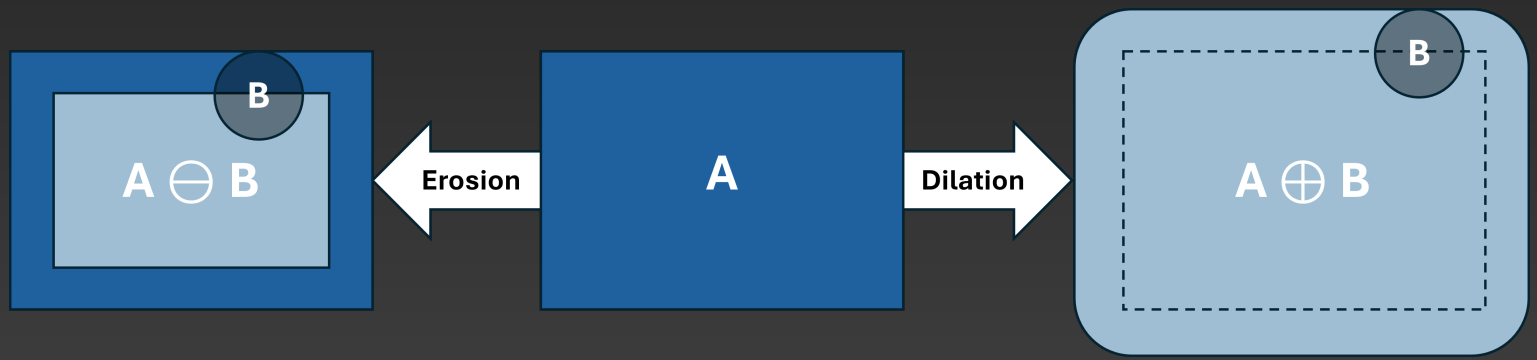

Illustration of Morphological Opening

- The morphological opening of image A by the structuring element B is denoted by

$$A \circ B = (A \ominus B) \oplus B$$

- Illustration of *morphological opening*

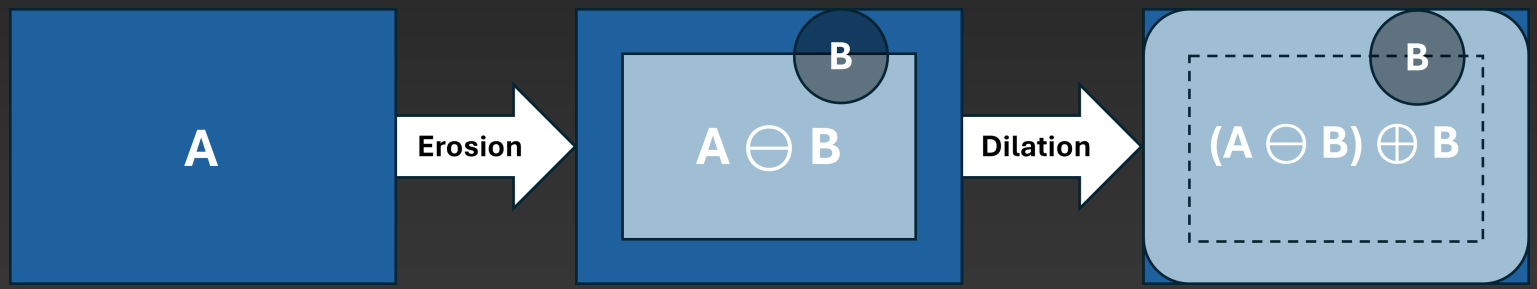

Application on the Mortality Improvement Surface

- The *erosion filter* first finds the local minima, under a disc-shaped neighboring window $\mathcal{C}$. The *dilation filter* is then applied to the local minima to obtain the local maxima.

$$\mathcal{Z}_{x,t} = max\{\, min\{\, \tilde{Z}_{x,t} \,|\, (x,t) \in \mathcal{C} \,\} \,|\, (x,t) \in \mathcal{C} \,\}$$

  - The point (x,t) is classified as nonground layer $\mathcal{NG}$ (a.k.a. Digital Surface Model "DSM") if $\mathcal{Z}_{x,t} > D$.
  - Otherwise, the point (x,t) is classified as ground layer $\mathcal{G}$ (a.k.a. Digital Terrain Model "DTM").

Application on the Mortality Improvement Surface

- The *erosion filter* first finds the local minima, under a disc-shaped neighboring window $\mathcal{C}$. The *dilation filter* is then applied to the local minima to obtain the local maxima.

$$\mathcal{Z}_{x,t} = max\{\, min\{\, \tilde{Z}_{x,t} \,|\, (x,t) \in \mathcal{C} \,\} \,|\, (x,t) \in \mathcal{C} \,\}$$

  - The point (x, t) is classified as nonground layer $\mathcal{NG}$ (a.k.a. Digital Surface Model "DSM") if $\mathcal{Z}_{x,t} > D$.
  - Otherwise, the point (x, t) is classified as ground layer $\mathcal{G}$ (a.k.a. Digital Terrain Model "DTM").

Application on the Mortality Improvement Surface

- The *erosion filter* first finds the local minima, under a disc-shaped neighboring window $\mathcal{C}$. The *dilation filter* is then applied to the local minima to obtain the local maxima.

$$\mathcal{Z}_{x,t} = max\{\, min\{\, \tilde{Z}_{x,t} \,|\, (x,t) \in \mathcal{C} \,\} \,|\, (x,t) \in \mathcal{C} \,\}$$

  - The point (x,t) is classified as nonground layer $\mathcal{NG}$ (a.k.a. Digital Surface Model "DSM") if $\mathcal{Z}_{x,t} > D$.
  - Otherwise, the point (x,t) is classified as ground layer $\mathcal{G}$ (a.k.a. Digital Terrain Model "DTM").

Computation of Normalized Elevation

- To extract the "pure" short-term effect from $\mathcal{G}$ and $\mathcal{NG}$.
- We create an estimated elevation of ground with interpolant,

$$G_{x,t} = \begin{cases} \tilde{Z}_{x,t}, & \text{if } (x,t) \in \mathcal{G} \\ g(\tilde{Z}_{x,t}), & \text{if } (x,t) \notin \mathcal{G} \end{cases}$$

  where $g(\tilde{Z}_{x,t})$ is the value from linear interpolation.
- The *normalized elevation* is then computed by

$$H_{x,t} = \tilde{Z}_{x,t} - G_{x,t} = \begin{cases} 0, & \text{if } (x,t) \in \mathcal{G} \\ \tilde{Z}_{x,t} - g(\tilde{Z}_{x,t}), & \text{if } (x,t) \notin \mathcal{G} \end{cases} \quad (2)$$

- $H_{x,t}$ is also known as Canopy Height Model (CHM).

Numerical Illustration

Data: U.S. males population, ages 60-89, years 1960-2019

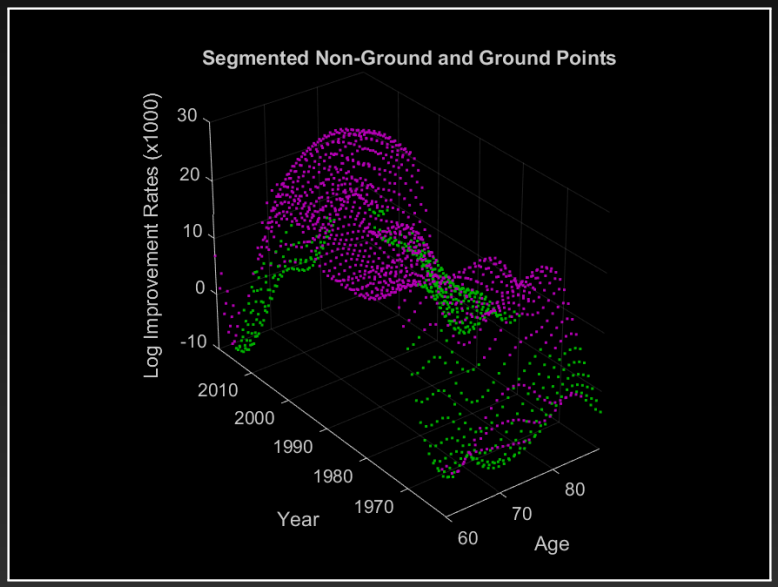

(a) Ground/Nonground

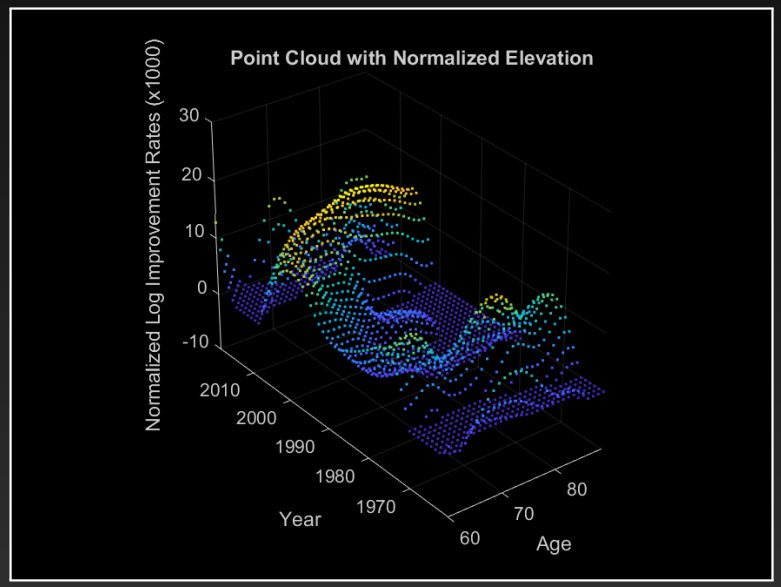

(b) Normalized Elevation

Figure: Segmentation of ground/nonground layer and the resulting normalized elevation.

A LiDAR Approach

Stage 3: Wave Tops Detection

Stage 3: Wave Tops Detection

- Adapts the method used for individual tree detection (e.g., Pitkänen et al., 2004) that finds local maxima within variable window sizes.
- Assumes a simple linear relationship between magnitude (or "height") and lasting period ("width") of the wave,

$$W_{x,t} = a + b * H_{x,t} \tag{3}$$

where

- $W_{x,t}$ represents the diameter of the shirt-term wave effects,
- a, the intercept, sets the baseline lasting period of a wave,
- b, the slope, describes how lasting period increases with respect to the magnitude of the wave.

Stage 3: Wave Tops Detection

- The radius of the variable window is then determined by rounding $W_{x,t}/2$ to the nearest integer.
  - For example, let us assume $a = 1$, $b = 0.2$, and $H_{x,t} = 11$.
  - We have $W_{x,t} = 1 + 0.2 \times 11 = 3.2$.
  - The radius of the variable window equals 2 since $3.2/2 = 1.6 \approx 2$.
- For each data point, we compare its value with the local maxima within the surrounding variable search window. If the local maxima is identical to the value of the data point, it will be identified as a wave top.

Numerical Illustration

Data: U.S. males population, ages 60-89, years 1960-2019

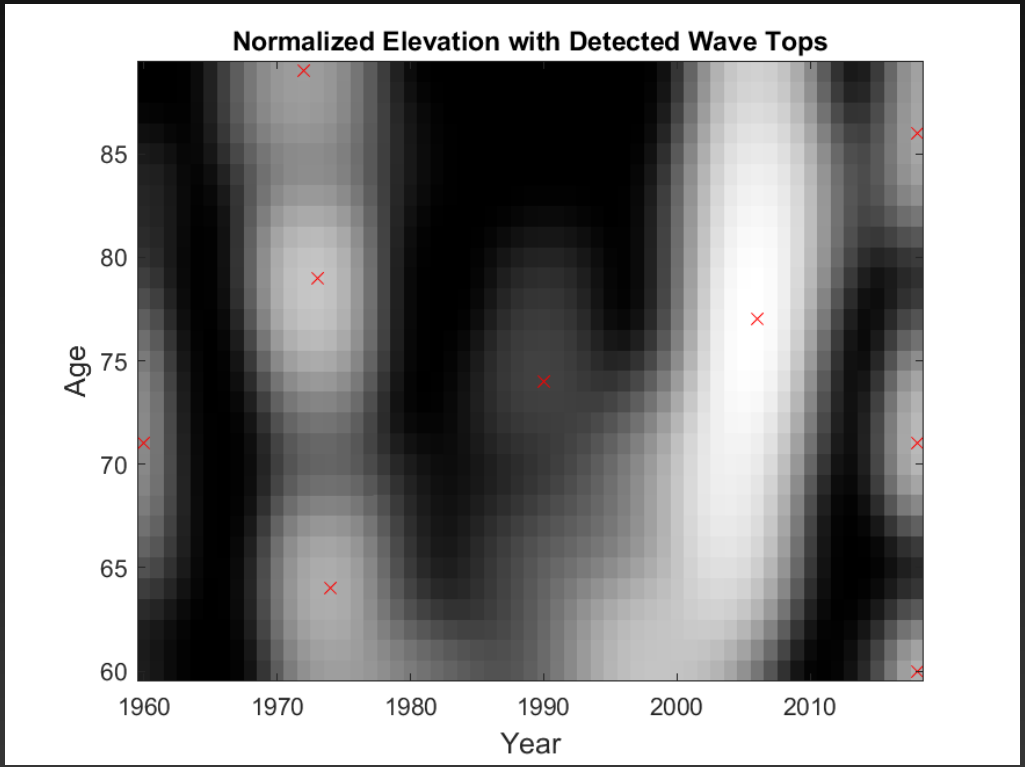

Figure: Grey-scale heat map of normalized elevation with detected wave tops.

A LiDAR Approach

Stage 4: Individual Wave Segmentation

Stage 4: Individual Wave Segmentation

- Each data point in $\mathcal{NG}$ will be assigned to one individual wave according to the detected wave tops.
- Watershed segmentation method is used.
- The idea is to mimic the flooding of basins.
  - When water is gradually poured into the bottoms, the basins start to fill up. When the water from different basins meet, boundaries are formed.

Illustration of the watershed segmentation method

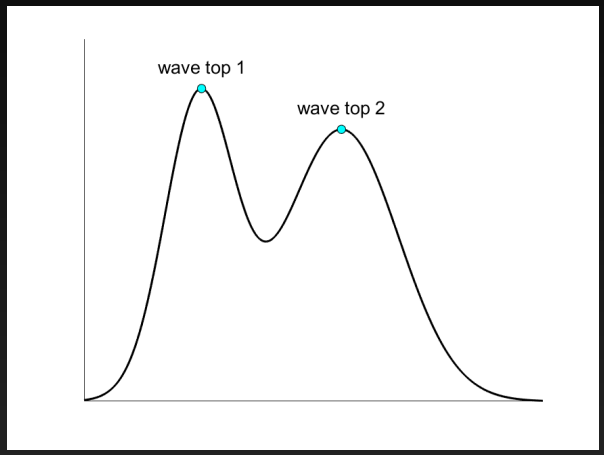

(a) Hypothetical Waves

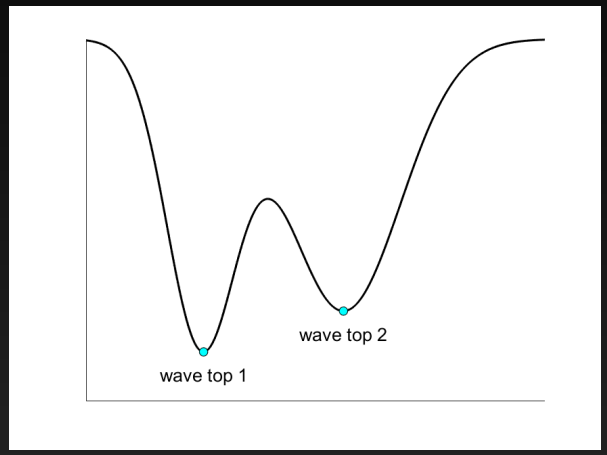

(b) Complement of Waves

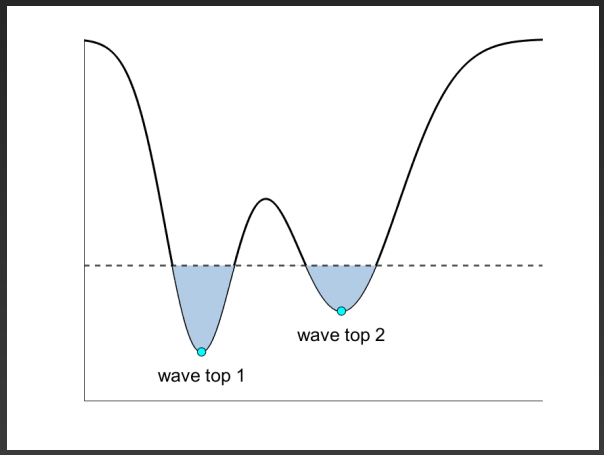

(c) Early Stage of Flooding

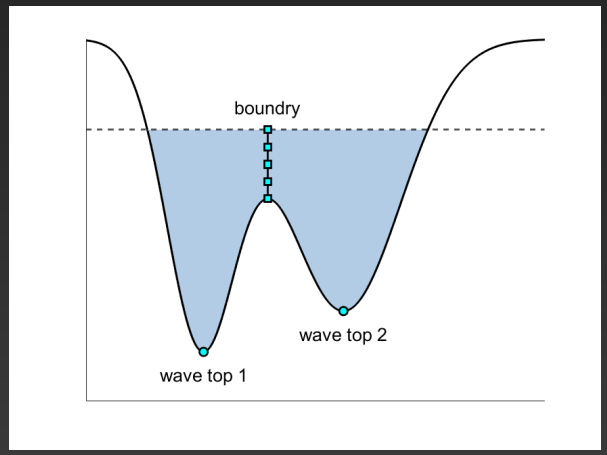

(d) Late Stage of Flooding

Marker-Controlled Watershed Segmentation

- The watershed method can lead to over-segmentation.
  - i.e., dividing into too many segments.
- We address this issue by the marker-controlled watershed segmentation method that utilizes the detected wave tops.
- Implementation:
  1. Compute the complement of normalized elevation,

$$C_{x,t} = (\max(H_{x,t}) - H_{x,t}), \tag{4}$$

  2. $C_{x,t}$ is filtered by *minima imposition*, which gives $R^{\varepsilon}_{\mathbf{C}\wedge\mathbf{M}}(\mathbf{M})$.
  3. Apply the watershed segmentation algorithm to $R^{\varepsilon}_{\mathbf{C}\wedge\mathbf{M}}(\mathbf{M})$

Marker-Controlled Watershed Segmentation

Minima Imposition

- Minima imposition (see Soille, 2003 and Chen et al., 2006)
  1. A marker image is created to highlight the wave tops

$$M_{x,t} = \begin{cases} 0, & \text{if } (x,t) \text{ is the detected wave top,} \\ C_{x,t}, & \text{otherwise.} \end{cases} \tag{5}$$

  2. Find the minimum between the mask image (i.e., $C_{x,t}$) and the marker image, $C_{x,t} \wedge M_{x,t}$
  3. Conduct morphological reconstruction by applying the morphological erosion of $(C_{x,t} \wedge M_{x,t})$ from $M_{x,t}$ iteratively until stability is reached.
- The minima-imposed result is denoted by $R^{\varepsilon}_{\mathbf{C} \wedge \mathbf{M}}(\mathbf{M})$.

Numerical Illustration

Data: U.S. males population, ages 60-89, years 1960-2019

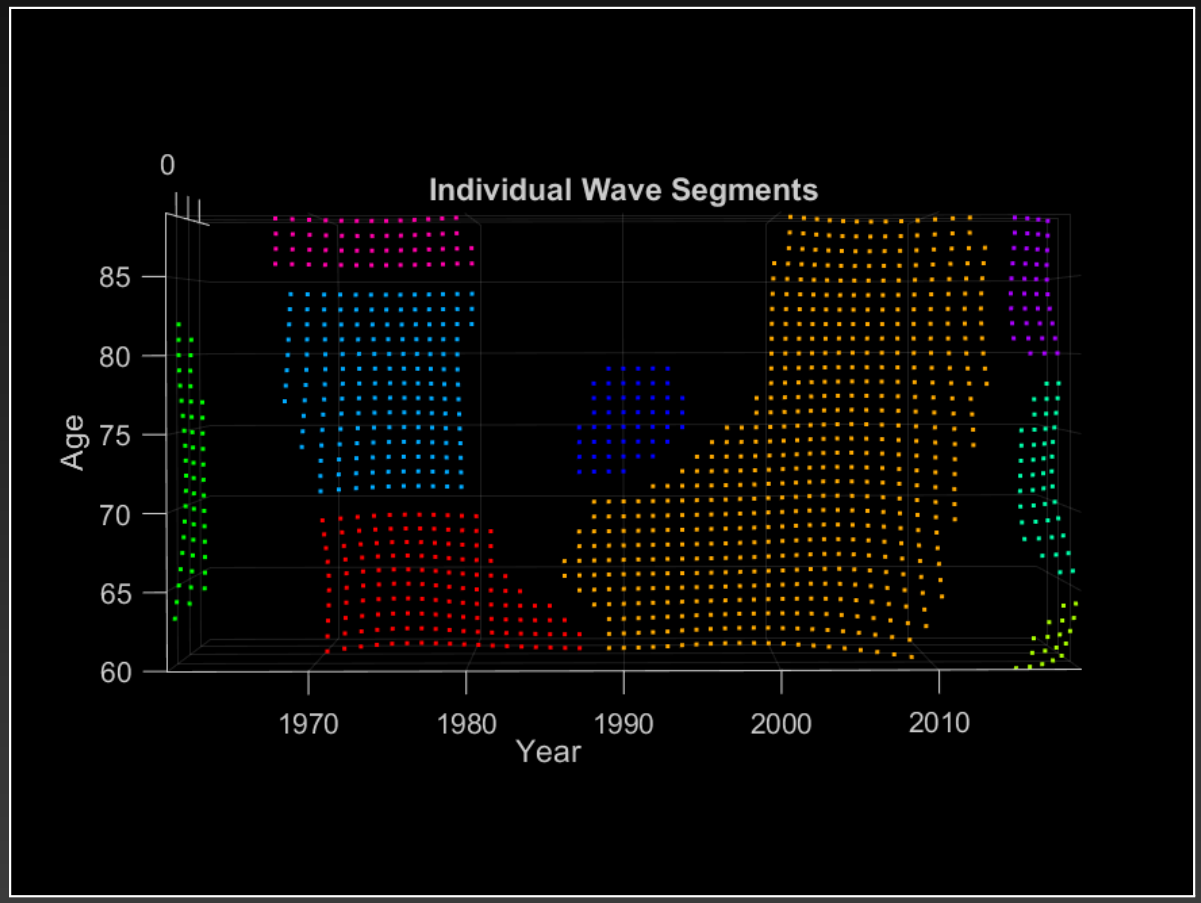

Figure: Segmentation of Individual Waves.

A LiDAR Approach

Stage 5: Fitting of Individual Waves

Stage 5: Fitting of Individual Waves

- Each wave segment is characterized by a 2-D surface.

$$f(x, t; \vec{\theta}) = \lambda \times \frac{1}{2\pi\sigma_{11}\sigma_{22}\sqrt{1-\rho^2}} \times \exp\left(-\frac{1}{2(1-\rho^2)}\left(\left(\frac{x-\hat{x}}{\sigma_{11}}\right)^2 - 2\rho\left(\frac{x-\hat{x}}{\sigma_{11}}\right)\left(\frac{t-\hat{t}}{\sigma_{22}}\right) + \left(\frac{t-\hat{t}}{\sigma_{22}}\right)^2\right)\right)$$

  where
  - λ captures the magnitude of short-term wave effects,
  - $\hat{x}$ and $\hat{t}$ denote the detected wave top location along the age and time dimension for this specific wave,
  - σ_{11} and σ_{22} control the lasting period of waves over age dimension and year dimension, respectively, and
  - ρ describes the their correlation along age/year dimension.

Numerical Illustration

Data: U.S. males population, ages 60-89, years 1960-2019

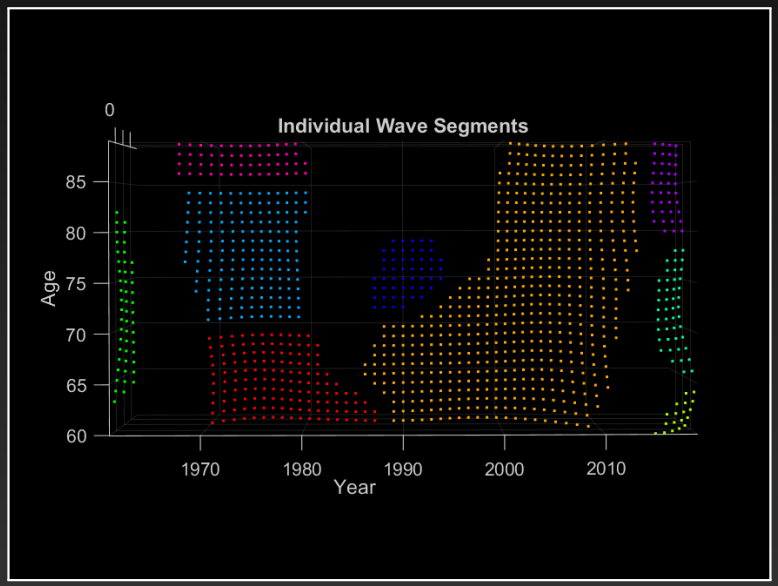

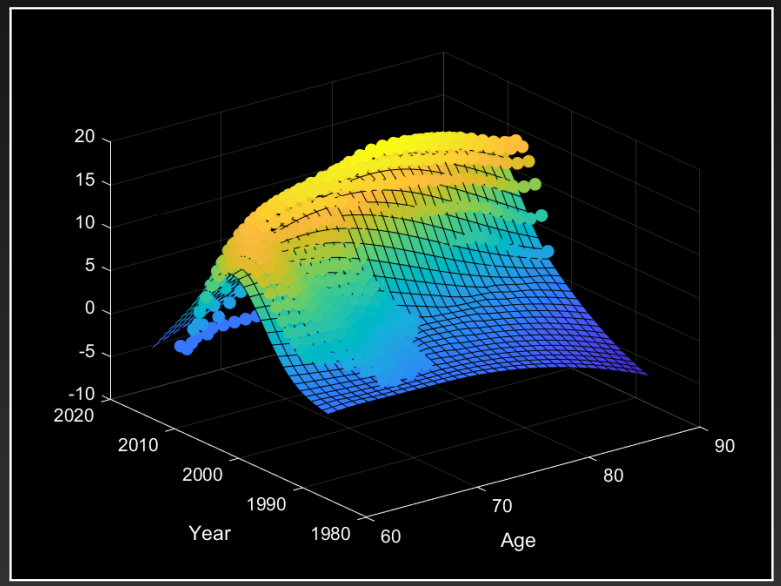

Figure: Fitting of Individual Waves (the orange segment)

Numerical Illustration

Data: U.S. males population, ages 60-89, years 1960-2019

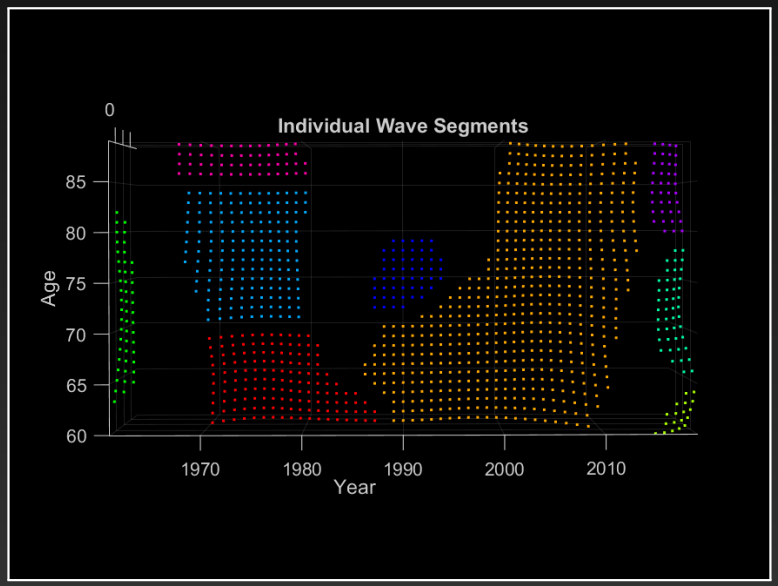

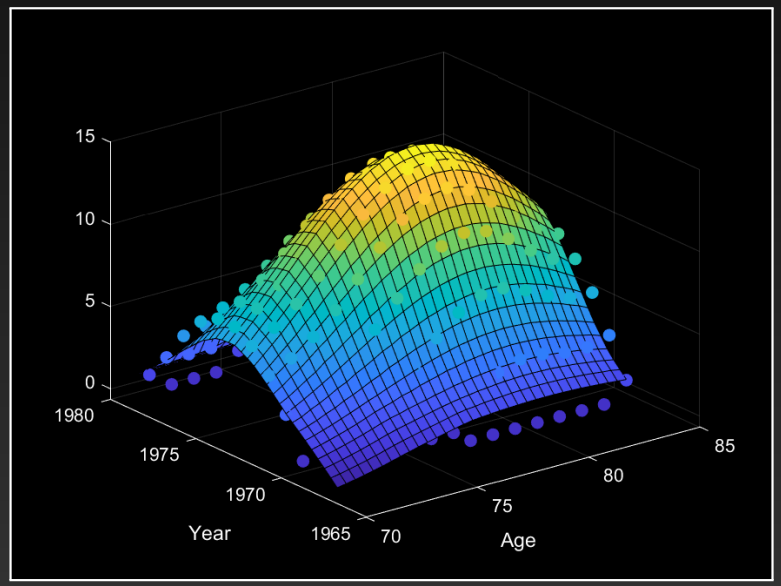

Figure: Fitting of Individual Waves (the light blue segment)

A LiDAR Approach

Stage 6: Identification of Long-term Improvement Rates

Stage 6: Identification of Long-term Improvement Rates

- The identified long-term background improvement layer is

$$\tilde{G}_{x,t} = \tilde{Z}_{x,t} - W^{(h)}_{x,t} + W^{(c)}_{x,t}$$

where

$$W^{(h)}_{x,t} = \sum_{j=1}^{N^{(h)}} f(\, x, t\,;\, \vec{\theta}^{(h)}_j\,),$$

is the collective short-term improvement, and

$$W^{(c)}_{x,t} = \sum_{j=1}^{N^{(c)}} f(\, x, t\,;\, \vec{\theta}^{(c)}_j\,),$$

is the collective short-term deterioration.

Numerical Illustration

Data: U.S. males population, ages 60-89, years 1960-2019

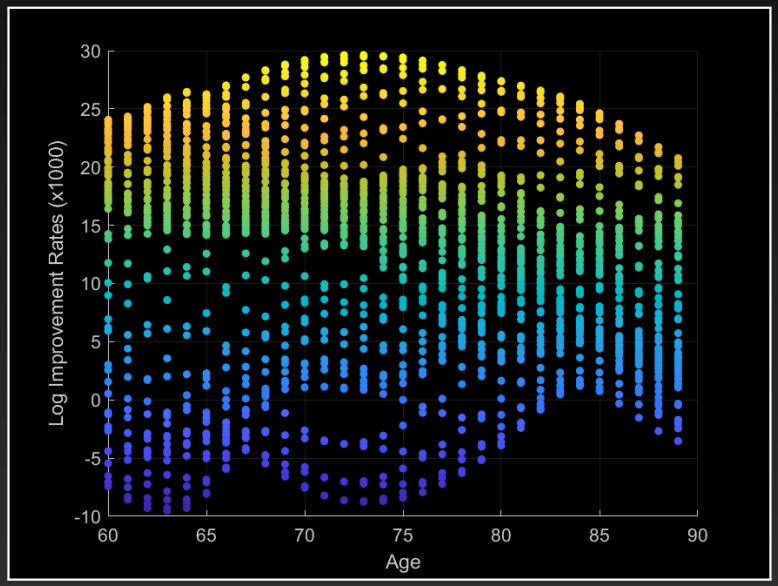

(a) Mortality Improvement Rates

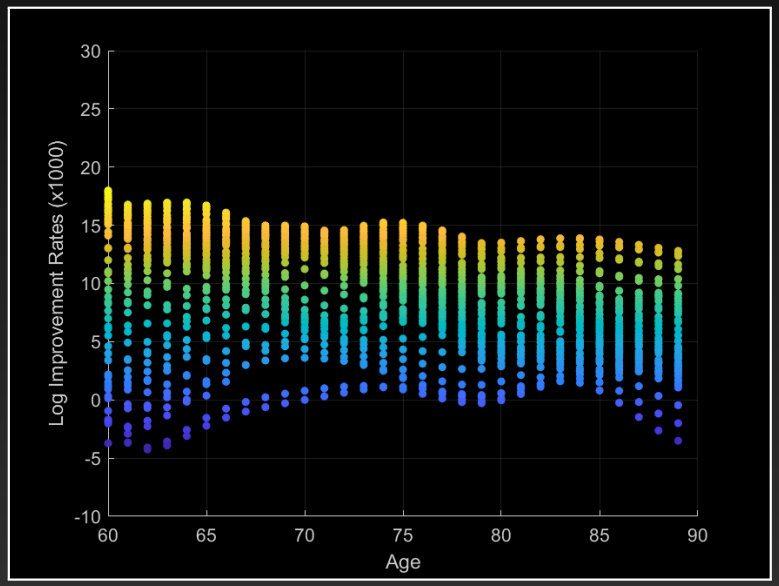

(b) Identified Ground Layer

Figure: Comparison between the smoothed mortality improvement rates ($\tilde{Z}_{x,t}$) and the retrieved ground layer ($\tilde{G}_{x,t}$) along the age axis.

Numerical Illustration

Data: U.S. males population, ages 60-89, years 1960-2019

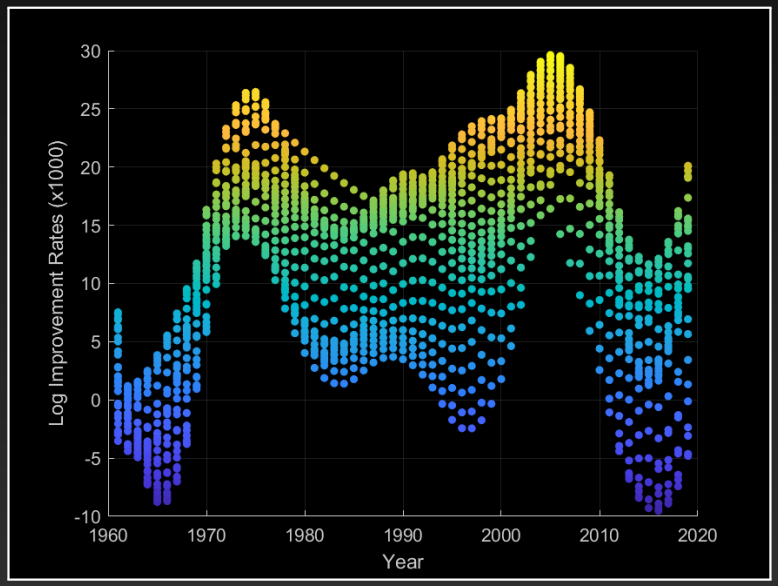

(a) Mortality Improvement Rates

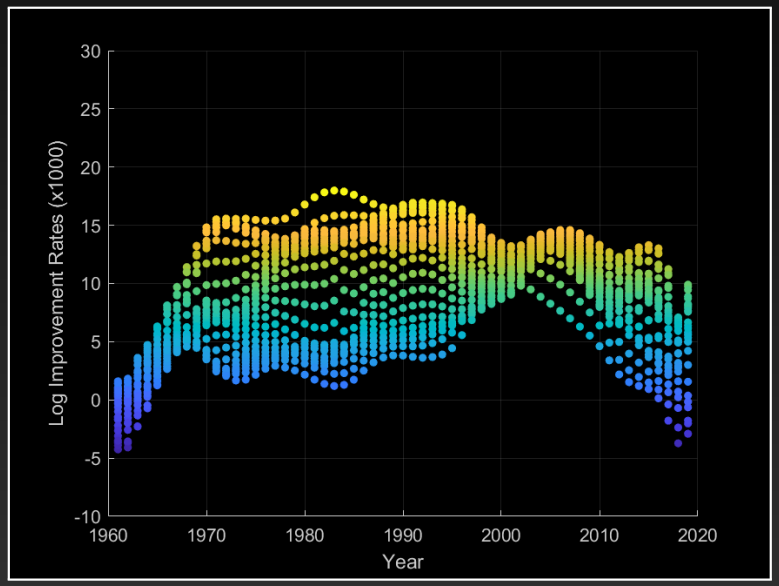

(b) Identified Ground Layer

Figure: Comparison between the smoothed mortality improvement rates ($\tilde{Z}_{x,t}$) and the retrieved ground layer ($\tilde{G}_{x,t}$) along the year axis.

Stage 6: Identification of Long-term Improvement Rates

Methods for the identification of long-term improvement rates:

- Method 1: A constant improvement rate for all ages/years.

$$\tilde{G}_{x,t} = \delta^{(1)} + e_{x,t} \tag{6}$$

- Method 2: A constant improvement rate across the time dimension, but with varying age effects b_x,

$$\tilde{G}_{x,t} = b_x \times \delta^{(2)} + e_{x,t} \tag{7}$$

- Method 3: The long-term improvement rate changes across both the time dimension and the age dimension,

$$\tilde{G}_{x,t} = b_x \times \delta_t^{(3)} + e_{x,t} \tag{8}$$

Stage 6: Identification of Long-term Improvement Rates

Methods for the identification of long-term improvement rates:

- Method 1: A constant improvement rate for all ages/years.

$$\tilde{G}_{x,t} = \delta^{(1)} + e_{x,t} \tag{6}$$

- Method 2: A constant improvement rate across the time dimension, but with varying age effects b_x,

$$\tilde{G}_{x,t} = b_x \times \delta^{(2)} + e_{x,t} \tag{7}$$

- Method 3: The long-term improvement rate changes across both the time dimension and the age dimension,

$$\tilde{G}_{x,t} = b_x \times \delta_t^{(3)} + e_{x,t} \tag{8}$$

Stage 6: Identification of Long-term Improvement Rates

- Base on the US male population (age 60-89, years 1960-2019), the KPSS test on $\delta_t^{(3)}$ indicate that this process is stationary.
- The optimal time series model for $\delta_t^{(3)}$ is selected via the AIC criterion.
- The long-term improvement rates for age x is calculated as follow:
  1. project $\delta_t^{(3)}$ to distant future
  2. multiply $\delta_t^{(3)}$ by the associated age-effects b_x

Numerical Illustration

Table: Long-term (average) mortality improvement rates from the LiDAR approach, MP-2021, and Lee-Carter (1992) model.

Age Range	LiDAR Approach	MP-2021	Lee-Carter Model
60 to 64	**1.19%**	1.34%	1.40%
65 to 69	**1.25%**	1.28%	1.44%
70 to 74	**1.16%**	1.21%	1.39%
75 to 79	**0.97%**	1.14%	1.25%
80 to 84	**0.77%**	1.01%	1.02%
85 to 89	**0.60%**	0.77%	0.73%

Concluding Remarks

- A 6-stage LiDAR approach is proposed for identifying long-term mortality improvement rates.
- The proposed LiDAR approach reveals the long-term background layer by removing the short-term effects of mortality improvement and deterioration.
- The volatility of the resulting long-term background layer is dramatically reduced along both age and year dimensions.
- Compared to MP-2021 and Lee-Carter model, the proposed LiDAR approach projects lower long-term mortality improvement rates.

References

- Chen, Q., Baldocchi, D., Gong, P., and Kelly, M. (2006) Isolating individual trees in a savanna woodland using small footprint lidar data. *Photogrammetric Engineering & Remote Sensing*, 72(8), 923-932.
- Currie I.D., Durban M., Eilers P.H. (2004) Smoothing and forecasting mortality rates. *Statistical Modelling.* 4(4):279-298.
- Lee, R. D., and Carter, L. R. (1992) Modeling and forecasting US mortality. *Journal of the American statistical association*, 87(419), 659-671.
- Li, J. S. H., and Liu, Y. (2020) The heat wave model for constructing two-dimensional mortality improvement scales with measures of uncertainty. *Insurance: Mathematics and Economics*, 93, 1-26
- Pingel, T.J., Clarke, K.C., and McBride, W.A. (2013) An improved simple morphological filter for the terrain classification of airborne lidar data. *ISPRS Journal of Photogrammetry and Remote Sensing*, 77:21-30.
- Pitkänen, J., Maltamo, M., Hyyppä, J., and Yu, X. (2004) Adaptive methods for individual tree detection on airborne laser based canopy height model. *International Archives of Photogrammetry, Remote Sensing and Spatial Information Sciences*, 36(8), 187-191.
- Soille, P. (2003) Morphological Image Analysis: Principles and Applications, 2nd Edition. Berlin: Springer.

Questions and Answers